Supporting Information

A Facile Strategy for Photoactive Nanocellulose-based Antimicrobial Materials

David Ramirez Alvarado,[a] Dimitris S. Argyropoulos,[b] Frank Scholle[c], Bharadwaja S.T. Peddinti[d] and Reza A. Ghiladi [a]*

Departments of [a]Chemistry, [b]Forest Biomaterials, [c]Biological Sciences, and [d]Chemical & Biomolecular Engineering, North Carolina State University, Raleigh, North Carolina 27695, USA

Table of Contents

Figure S1. Representative colony-counting data (TSB-agar plates) obtained for the photodynamic inactivation studies employing 5 μM **A_3B^{3+}-NFC** against methicillin-resistant *S. aureus* ATCC-44 (MRSA).

Figure S2. Scanning electron microscopy images of (A) unmodified freeze-dried NFC and (B) **A_3B^{3+}-NFC**.

Photosensitizer singlet oxygen quantum yield (Φ_Δ) determination.

Table S1. Singlet oxygen quantum yield values (Φ_Δ) as determined by time-resolved phosphorescence measurements in D_2O.

Figure S3. ATR-IR spectra of **A_3B^{3+}** (**3**) and **ZnA_3B^{3+}** (**4**).

LIVE/DEAD Bacterial Viability Assays

Figure S4. Confocal laser scanning microscopy images of a) material-free cells only (live control), (b) *S. aureus* cells exposed to ethanol (dead control), (c) *S. aureus* cells exposed to A_3B^+-NFC kept in dark (material-present dark control), and (d-f) *S. aureus* cells exposed to **A_3B^+-NFC** illuminated at 65 ± 5 mW/cm^2.

Solution Based Antimicrobial Activity of A_3B^{3+} (3) and ZnA_3B^{3+} (4).

Figure S5. Solution-based photodynamic inactivation studies of *K. pneumoniae* using **A_3B^{3+}** and **ZnA_3B^{3+}** as photosensitizers.

Without illumination

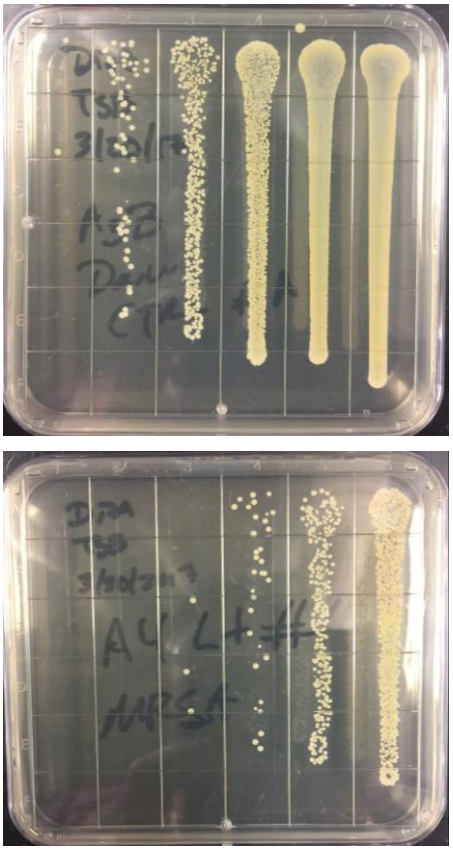

With illumination

Figure S1. Representative colony-counting data (TSB-agar plates) obtained for the photodynamic inactivation studies employing 5 μM **A_3B^{3+}-NFC** against methicillin-resistant *S. aureus* ATCC-44 (MRSA): *top panel*, without illumination (material-present dark control); *bottom panel*, illuminated study (60 min, 400–700 nm, 65 ± 5 mW/cm^2). Each vertical column represents a 1:10 serial dilution, with increasing dilution from right to left.

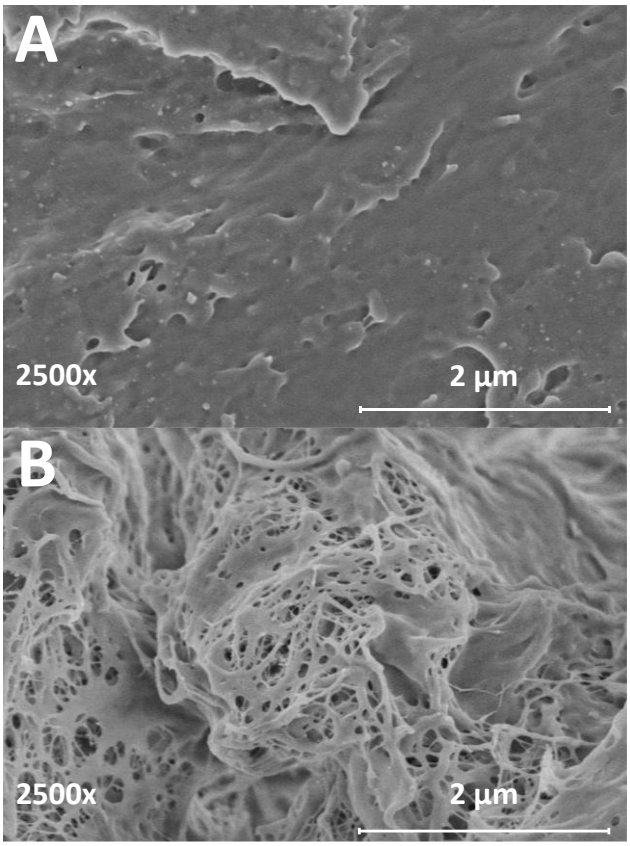

Figure S2. Scanning electron microscopy images of (A) unmodified freeze-dried NFC and (B) **A_3B^{3+}-NFC**.

Photosensitizer singlet oxygen quantum yield (Φ_Δ) determination by time-resolved phosphorescence measurements. Time-resolved singlet oxygen phosphorescence experiments were conducted in D_2O to determine singlet oxygen quantum yield (Φ_Δ) values for (**3**) and (**4**) using TMPyP as the standard (Φ_Δ=0.74[1]). Singlet oxygen quantum yield determination relies on its phosphorescence at 1270 nm and by quantitatively comparing emission intensities of optically-equivalent photosensitizer and standard solutions. Samples were prepared to equal absorbance values (0.31) at the excitation wavelength of 433 nm. Due to the weak nature of the $^1O_2$ phosphorescence emission band at 1270 nm, sample excitation at 433 nm and emission bandwidth data were performed with a 20 nm (433±10 nm) bandwidth. Emission intensities were baselined and integrated from 1225 and 1325 nm. The $^1O_2$ quantum yield values were calculated according to the following equation:

$$Q = Q_R \frac{I}{I_R} \frac{OD_R}{OD} \quad \text{and} \quad OD = 1 - 10^{-Abs} \qquad \text{Eq. 1}$$

where the integrated singlet oxygen phosphorescence intensity is represented by I, and OD is the optical density at the excitation wavelength, or range; R refers to the reference photosensitizer, TMPyP.[2]

Table S1. Singlet oxygen quantum yield values (Φ_Δ) as determined by time-resolved phosphorescence measurements in D_2O.

	Φ_Δ (D_2O)
A_3B^{3+} (**3**)	0.044[a]
ZnA_3B^{3+} (**4**)	0.156[a]

[a]TMPyP (Φ_Δ=0.74) was used as reference PS for $^1O_2$ quantum yield measurements.[1]

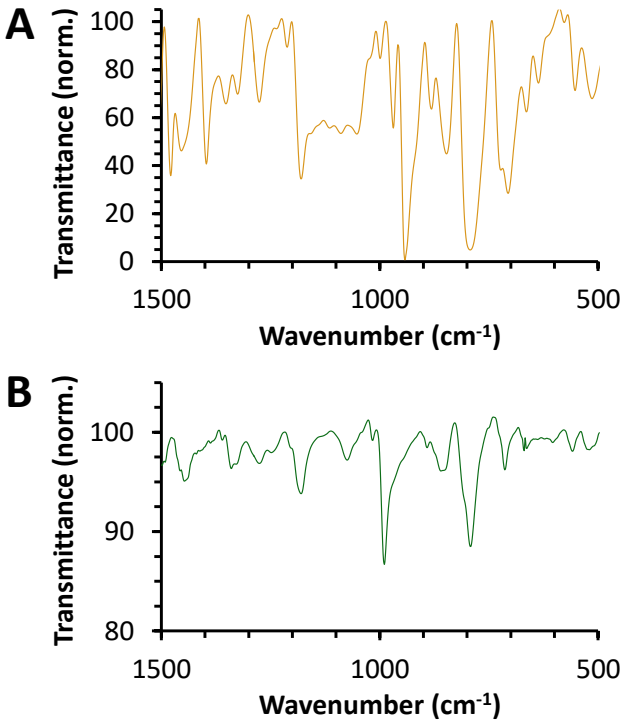

Figure S3. ATR-IR spectra of $\mathbf{A_3B^{3+}}$ (**3**) and $\mathbf{ZnA_3B^{3+}}$ (**4**).

LIVE/DEAD Bacterial Viability Assays

Confocal laser scanning microscopy was performed to image *S. aureus* (ATCC-2913) after staining the cells with a LIVE/DEAD *Bac*Light Bacterial Viability and Counting Kit that consisted of green-fluorescent SYTO9 and red-fluorescent propidium iodide (PI) stains As shown in Figure S4, samples included: (A) compound free *S. aureus* cells only that served as a live control, (B) *S. aureus* cells washed with ethanol that served as a dead control, (C) *S. aureus* cells exposed to **A_3B^+-NFC** and kept in the dark that served as dark control, and (D-F) *S. aureus* cells exposed to **A_3B^+-NFC** that were illuminated by non-coherent visible light at 65 $\pm$ 5 mW/cm^2. A 5 μM solution of the **A_3B^+-NFC** was used for the dark control and the illuminated samples. Initially, the cells were separated from phosphate buffer saline (PBS) via centrifugation. Subsequently, the cells were washed with 0.9 % w/v sodium chloride (NaCl). Following this, the cells were resuspended in 0.9 % w/v NaCl, and a premix of SYTO9 : propidium iodide (1:1) was added. The cells were then vortexed, incubated at room temperature for 30 min, and then a few microliters of the stained cell solution were taken in a glass holder added with a coverslip and imaged with a Zeiss LSM 880 confocal microscope (NC State University Cellular and Molecular Imaging Facility, NSF grant DBI-1624613). Live cells possessing intact cell membranes are stained bright green by SYTO9, whereas the dead cells with the ruptured/damaged cell membranes are stained red and exhibit less/negligible green fluorescence. As seen in Figure S4, the fluorescent images for the material-free control (Figure S4A) and the material-present cells kept in the dark (Figure S4C) both show significantly higher number of live cells. As expected, the light illuminated samples (Figure S4D-F) only show dead cells, comparable to the ethanol treated dead control (Figure S4B), demonstrating that **A_3B^+-NFC** is bactericidal when illuminated.

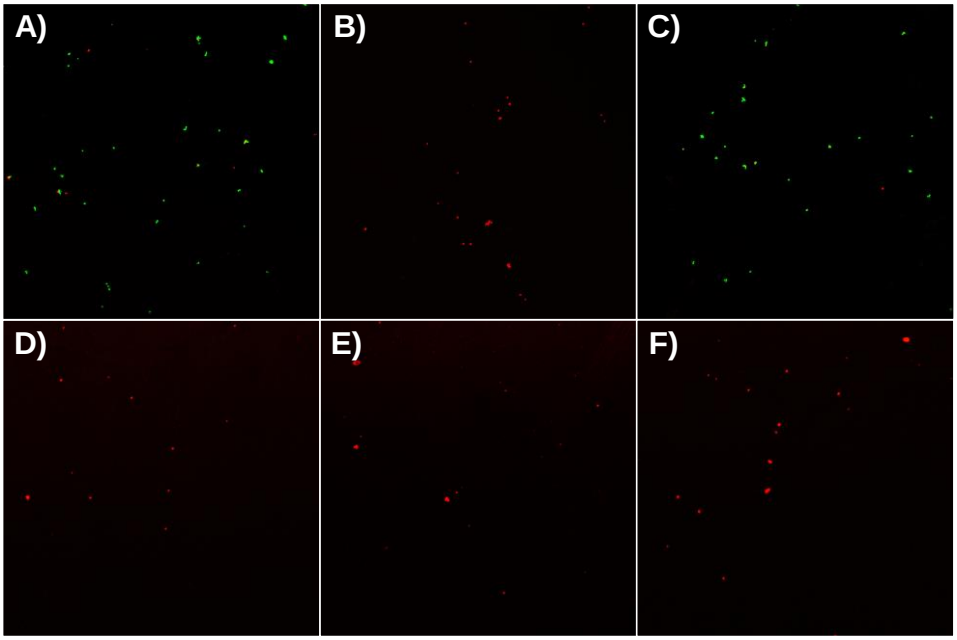

Figure S4. Confocal laser scanning microscopy images of A) material-free cells only (live control), B) *S. aureus* cells exposed to ethanol (dead control), C) *S. aureus* cells exposed to A_3B^+-NFC kept in dark (material-present dark control), and D-F) *S. aureus* cells exposed to **A_3B^+-NFC** illuminated at 65 ± 5 mW/cm^2 for 60 minutes, 400-700 nm.

Solution Based Antimicrobial Activity of A_3B^{3+} (3) and ZnA_3B^{3+} (4). Solution studies comparing the antimicrobial efficacy of freebase **A_3B^{3+}** (**3**) and metallated **ZnA_3B^{3+}** (**4**) porphyrins in the inactivation of *K. pneumoniae* (KP), the least susceptible to PDI of the two Gram-negative strains in this study, were conducted (**Figure S3**). An initial test of **A_3B^{3+}** at a 1 μM concentration resulted in no antimicrobial activity against KP, thus a higher concentration, 2.5 μM, was pursued. Inactivation studies at 2.5 μM concentrations revealed a 98.2734% ($P < 0.0001$) and 99.9991% ($P = 0.0002$) reduction in *K. pneumoniae* for **A_3B^{3+}** and **ZnA_3B^{3+}** respectively. Studies conducted at 5 μM yielded a 99.9996% ($P < 0.0001$) and 99.9999% ($P = 0.0004$) reduction in KP for **A_3B^{3+}** and **ZnA_3B^{3+}**. The metallated macrocycle exhibited a greater degree of PDI activity, as was expected, due to the heavy atom effect, which increases excited triplet state quantum yields toward singlet oxygen generation.

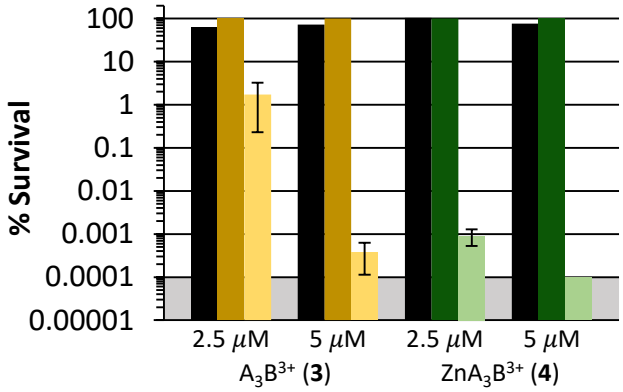

Figure S5. Solution-based photodynamic inactivation studies of *K. pneumoniae* using **A_3B^{3+}** (**3**) and **ZnA_3B^{3+}** (**4**) as photosensitizers. Displayed are the compound-free (cells-only) control (black bars), as well as the dark controls of **A_3B^{3+}** (dark yellow) and **ZnA_3B^{3+}** (dark green), and the illuminated studies of **A_3B^{3+}** (light yellow) and **ZnA_3B^{3+}** (light green) displayed as the percent survival of the compound-free control. The illumination conditions were as follows: 60 min, 400 −700 nm, 65 ± 5 mW/cm^2. As the plating technique employed to determine % survival did not allow for detection of survival rates of <0.0001%, data points below the detection limit were set to 0.0001% survival for graphing purposes and are indicated by the grey shaded area.

References

1. X. Ragàs, D. Sánchez-García, R. Ruiz-González, T. Dai, M. Agut, M. R. Hamblin and S. Nonell, *Journal of Medicinal Chemistry*, 2010, **53**, 7796-7803.
2. Joseph R. Lakowicz, *Principles of Fluorescence Spectroscopy*, Kluwer Academic/Plenum Publishers, New York, 2nd edn., 1999.